ACS APPLIED MATERIALS & INTERFACES

Research Article

www.acsami.org

Benzo[*a*]carbazole-Based Donor–π–Acceptor Type Organic Dyes for Highly Efficient Dye-Sensitized Solar Cells

Xing Qian,[†] Yi-Zhou Zhu,*[,†] Wen-Ying Chang,[†] Jian Song,[‡] Bin Pan,[†] Lin Lu,[†] Huan-Huan Gao,[†] and Jian-Yu Zheng*[,†]

[†]State Key Laboratory and Institute of Elemento-Organic Chemistry, Collaborative Innovation Center of Chemical Science and Engineering (Tianjin), Nankai University, Tianjin 300071, China

[‡]School of Materials Science and Engineering, China University of Mining and Technology, Xuzhou 221116, China

Supporting Information

ABSTRACT: A novel class of metal-free organic dyes based on benzo[*a*]carbazole have been designed, synthesized, and used in dye-sensitized solar cells for the first time. These types of dyes consisted of a cyanoacrylic acid moiety as the electron acceptor/anchoring group and different electron-rich spacers such as thiophene (**JY21**), furan (**JY22**), and oligothiophene (**JY23**) as the π-linkers. The photophysical, electrochemical, and photovoltaic properties, as well as theoretical calculations of these dyes were investigated. The photovoltaic performances of these dyes were found to be highly relevant to the π-conjugated linkers. In particular, dye **JY23** exhibited a broad IPCE response with a photocurrent signal up to about 740 nm covering the most region of the UV–visible light. A DSSC based on **JY23** showed the best photovoltaic performance with a J_{sc} of 14.8 mA cm^{-2}, a V_{oc} of 744 mV, and a FF of 0.68, achieving a power conversion efficiency of 7.54% under standard AM 1.5 G irradiation.

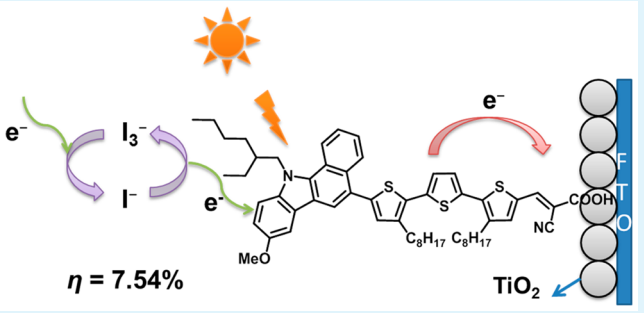

KEYWORDS: *dye-sensitized solar cells, organic dyes, benzo[a]carbazole, conjugated linkers, intramolecular charge transfer*

INTRODUCTION

Solar energy is very attractive because of its unlimited supply compared to other renewable energy resources. As an effective device for sunlight-to-electricity conversion, dye-sensitized solar cells (DSSCs) have been extensively investigated owing to their high theoretical power conversion efficiency (PCE), facile preparation processes, and potential low cost.[1,2] So far, ruthenium(II) polypyridyl complexes still stand out as highly efficient and stable sensitizers with a PCE of over 11%.[3] However, the high cost and toxicity of these Ru(II) sensitizers may limit their widespread applications in DSSCs. Recently, DSSC devices employing zinc-porphyrin sensitizers have achieved efficiency records exceeding 12% by using the Co^{II}/Co^{III} electrolyte under standard conditions.[4−6] From the viewpoint of practical application, the tedious synthetic procedures and low yield of porphyrin sensitizers will restrict their further use in DSSCs. On the other hand, metal-free organic dyes have, therefore, attracted considerable attention for the practical advantages, such as facilely structural modification, easy preparation, and low cost.[7]

Carbazole derivatives have been widely employed as active ingredients in organic light-emitting diodes (OLEDs),[8,9] organic photovoltaic cells (OPVs),[10] and DSSCs[11−14] due to their unique electronic and optical properties, and pronounced thermal stability. The existence of the many modification sites of carbazole makes it an attractive building block for functional group incorporation, and carbazole has been used in DSSCs both as a peripheral donor and a π-linker.[15] When carbazole is fused with a benzene ring to form benzo[*a*]carbazole, as a π-extended carbazole derivative, benzo[*a*]carbazole may have strong electron delocalization and significant potential for intramolecular charge transfer (ICT). To the best of our knowledge, the photovoltaic application of benzo[*a*]carbazole derivatives has not been reported yet. Herein, we have designed and synthesized a series of metal-free organic dyes containing benzo[*a*]carbazole acting as the electron donor and cyanoacrylic acid acting as the electron acceptor/anchoring group. In general, organic dyes configured with donor–π–acceptor (D–π–A) structures are strongly desirable for enabling efficient photoinduced charge separation.[16−20] An electron-rich π-conjugated linker is preferable to induce efficient ICT and extend spectral response to low energy solar photons for its better electron delocalization over the whole molecule, which facilitates donor–acceptor interactions.[21] So, we chose electron-rich spacers thiophene (**JY21**), furan (**JY22**), and

Received: November 29, 2014
Accepted: April 15, 2015
Published: April 15, 2015

DOI: 10.1021/am508400a
ACS Appl. Mater. Interfaces 2015, 7, 9015−9022

oligothiophene (**JY23**) to act as the π-linkers. The chemical structures of the three dyes are displayed in Figure 1.

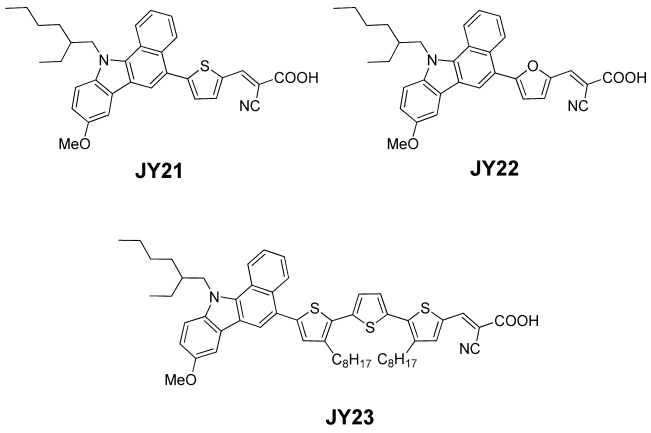

Figure 1. Chemical structures of **JY21**, **JY22**, and **JY23**.

RESULTS AND DISCUSSION

Dye Synthesis. Dyes **JY21**–**23** were synthesized by a concise synthetic procedure presented in Scheme 1. Benzo[*a*]-

Scheme 1. Synthetic Route for JY21, JY22, and JY23

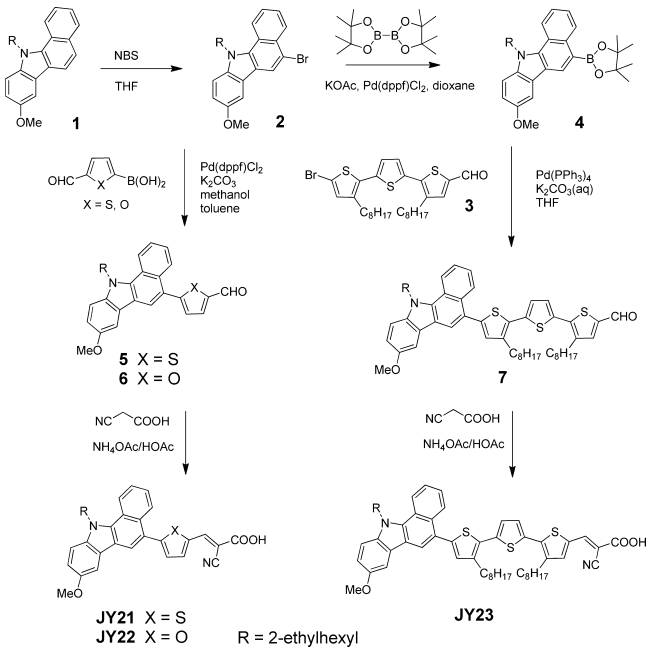

carbazole derivatives **1** and **2**, as well as oligothiophene **3**, were prepared according to literature procedures.[22−24] Coupling compound **2** with bis(pinacolato)diboron gave intermediate **4** containing borate group. Suzuki cross-coupling reaction was subsequently used to produce the π-extended benzo[*a*]-carbazole-based aldehydes **5**–**7** with intermediates **2** or **4** and indicated aromatic aldehydes. Finally, the precursors **5**, **6**, and **7** reacted with cyanoacetic acid via Knoevenagel condensation to afford **JY21**, **JY22**, and **JY23**, respectively.

UV−Visible Absorptions and Electrochemical Measurements. UV−vis absorption spectra were measured to investigate the photophysical properties of **JY21**, **JY22**, and **JY23**. Figure 2 depicts the UV−vis spectra of the dyes **JY21**–**23**

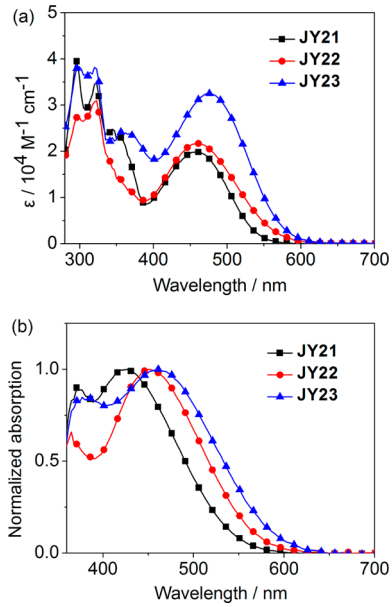

Figure 2. UV−vis absorptions of **JY21**–**23** (a) in dichloromethane and (b) on TiO_2 films.

in dichloromethane solutions and on TiO_2 surfaces. Table 1 summarizes the data of the UV−vis absorptions and electrochemical measurements of the three dyes. As shown in Figure 2a, the three dyes present two major absorption regions in dichloromethane solutions. The high-energy region at 280−400 nm can be attributed to π−π^* or n−π^* electron transitions of the molecular backbone, while the low-energy region at 400−600 nm with stronger intensity can be ascribed to the ICT transitions.[25] The maximum absorptions (λ_{max}) of **JY21**–**23** appear at 458, 462, and 477 nm, respectively. Obviously, the longest conjugated length in **JY23** (ε = 32 400 M^{-1} cm^{-1}) significantly red-shifts its ICT absorption band and enhances its molar extinction coefficient in comparison to **JY21** (ε = 20 200 M^{-1} cm^{-1}) and **JY22** (ε = 21 500 M^{-1} cm^{-1}). The results reveal that the expansion of electron-rich conjugated π-linkers can not only facilitate the interactions between donor and acceptor in dipolar molecules but also decrease the energy gap of the organic dyes. With regard to the spectra on TiO_2 films, the absorption peaks of the dyes are more blue-shifted than that in dichloromethane (Figure 2b). The blue-shifted absorption might result from the deprotonation of the carboxylic acid unit when the dyes were adsorbed on the TiO_2 surface.[26] It is interesting to compare the absorption features of benzo[*a*]-carbazole-based dyes with carbazole-based dyes with similar constructing method. As compared to the reported carbazole-based dyes **JK-24**,[27] **JK-28**,[27] **9a**,[15] and **9b**[15] with one thiophene linker (Figure 3), the maximum absorption peak (either in solution or on TiO_2 film) of the present dye **JY21** is obviously red-shifted. Similarly, the absorption red-shifts of dyes **JY22** and **JY23** were found in comparison to the analogous dyes **K2**[28] and **CCT3A**,[29] respectively. This should come from the fused benzene ring, benzo[*a*]carbazole, as a π-extended carbazole derivative, expands its electron delocalization and has a more significant potential for ICT.

Cyclic voltammetry measurements of the three dyes were performed in dichloromethane solutions with a scan rate of 100 mV s^{-1} (calibrated by ferrocene, 0.63 V vs normal hydrogen electrode (NHE)).[30] Cyclic voltammograms of the three dyes are depicted in Figure 4, and the corresponding energy levels

DOI: 10.1021/am508400a
ACS Appl. Mater. Interfaces 2015, 7, 9015−9022

Table 1. Photophysical and Electrochemical Data of JY21−23[a]

dye	λ_{max} (nm)	ε (10^4 M^{-1} cm^{-1})	λ_{max} (TiO_2) (nm)	E_{ox} (V)	E_{0-0} (V)	E_{red} (V)
JY21	458	2.02	428	1.22	2.16	−0.94
JY22	462	2.15	452	1.15	2.07	−0.92
JY23	477	3.24	461	0.99	1.98	−0.99

[a]First oxidation potentials (vs normal hydrogen electrode (NHE)) were measured in dichloromethane. E_{0-0} values were calculated from the onset wavelength of the absorption spectra in dichloromethane. $E_{red} = E_{ox} - E_{0-0}$.

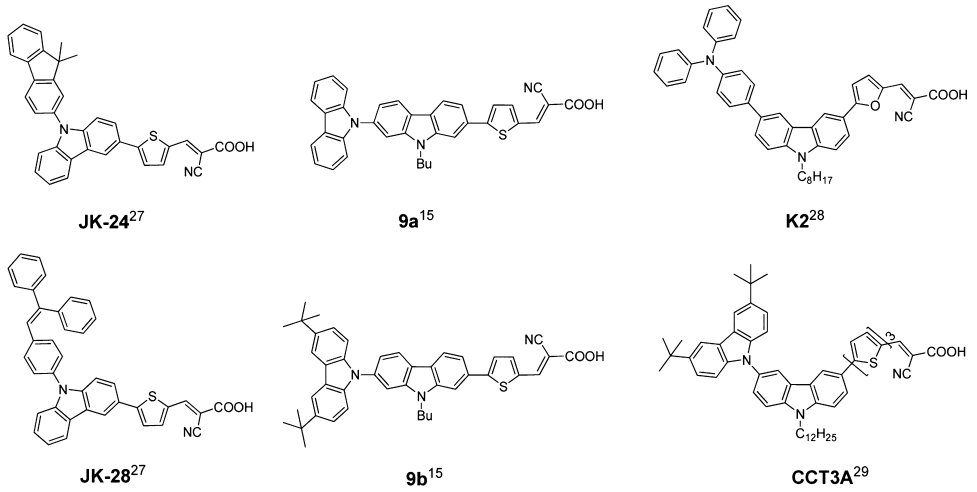

Figure 3. Chemical structures of the similar carbazole-based dyes.

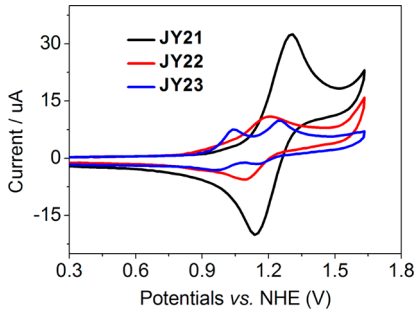

Figure 4. Cyclic voltammograms of **JY21−23**.

are provided in Figure 5. As shown in Figure 4, **JY21** and **JY22** both exhibited one reversible oxidation couple, while two reversible oxidation couples were observed for **JY23**. The first oxidation potentials (E_{ox}) of **JY21−23** corresponding to their highest occupied molecular orbital (HOMO) levels are evaluated to be 1.22, 1.15, and 0.99 V (vs NHE), respectively.

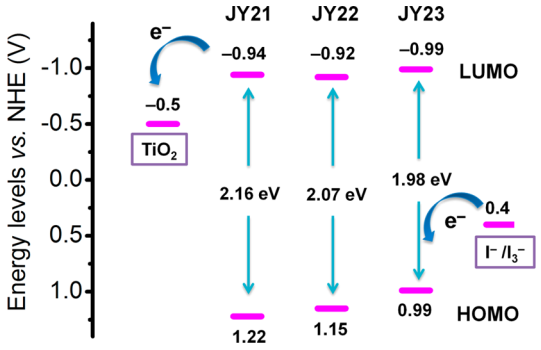

Figure 5. Energy levels of the three dyes as determined by cyclic voltammetry.

The band gap energies (E_{0-0}) of **JY21−23**, which can be estimated from the onset wavelength of their absorption spectra, are calculated to be 2.16, 2.07, and 1.98 eV, respectively. The lowest unoccupied molecular orbital (LUMO) levels of **JY21−23** (calculated from $E_{ox} - E_{0-0}$) are found to be −0.94, −0.92, and −0.99 V (vs NHE), respectively. As a result, the LUMO levels of **JY21−23** are more sufficiently negative than the conduction band (CB) of TiO_2 (−0.5 V vs NHE), energetically allowing electron injection from the excited dyes into the TiO_2 semiconductor. While the HOMO levels of **JY21−23** are much more positive than the iodide/triiodide redox couple (0.4 V vs NHE), which guarantees the regeneration of the oxidized dyes.

Computational Analysis. To investigate the frontier molecular orbitals of **JY21−23**, we performed theoretical calculations based on density functional theory (DFT) with Gaussian 03 package at the B3LYP/6-31G* level. The electron distributions of the HOMOs and LUMOs of **JY21−23** are shown in Figure 6. With regard to the HOMO states of the three dyes, the electron density is primarily distributed on the benzo[*a*]carbazole skeleton and nearby π-linkers. At the same time, the LUMOs of these dyes localize electron distributions from the cyanoacrylic acid moiety to nearby linkers because the ICT process happens along the π-linkers. This type electron distribution of the HOMOs and LUMOs of **JY21−23** indicates that HOMO−LUMO excitation moves the electron from benzo[*a*]carbazole donor to cyanoacrylic acid acceptor through the π-linker groups, ensuring efficient charge separation, and electron injection.

DSSC Performances. The photovoltaic performances of the DSSCs based on **JY21−23** under standard conditions (AM 1.5G, 100 mW cm^{-2}) were measured using an iodine electrolyte. The DSSCs data of **JY21−23**, **N719** dye, and analogous carbazole dyes are summarized in Table 2. The photocurrent density−voltage ($J-V$) curves of **JY21−23** are

DOI: 10.1021/am508400a
ACS Appl. Mater. Interfaces 2015, 7, 9015−9022

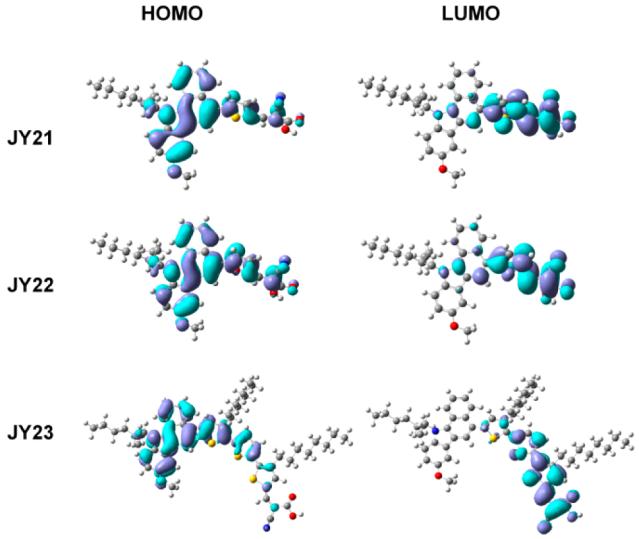

Figure 6. Electron distributions of the frontier orbitals of **JY21**–**JY23**.

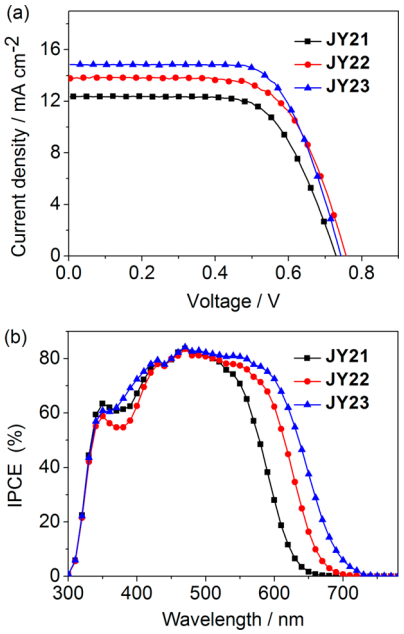

Figure 7. (a) The photocurrent density–voltage (J–V) curves and (b) the IPCE spectra of **JY21**–**23**.

plotted in Figure 7. A DSSC based on **JY21** with a thiophene as the π-linker gave a short-circuit photocurrent density (J_{sc}) of 12.4 mA cm^{-2}, an open-circuit photovoltage (V_{oc}) of 729 mV, a fill factor (FF) of 0.66, and a PCE of 6.01%. When the π-bridge of **JY21** was replaced by furan, the resultant **JY22**-based cell (V_{oc}: 757 mV; J_{sc}: 13.8 mA cm^{-2}) showed a significant improvement of V_{oc} and J_{sc} and finally gave a higher efficiency of 6.93% with a FF of 0.66. Notably, because of much broader and stronger ICT absorption, **JY23** displayed a highest J_{sc} of 14.8 mA cm^{-2}, a moderate V_{oc} of 744 mV, and an increased PCE of 7.54%. It should be pointed out that the increase of conjugation skeleton will broaden the absorption spectrum of the dyes and meantime lead to undesirable self-aggregation. This self-aggregation can induce serious self-quenching of excited dyes and finally give a low efficiency. Therefore, two alkyl substituents of **JY23** are very helpful to guarantee a high efficiency. The highest PCE of **JY23** reached about 94% of the **N719**-based cell measured under the same conditions, illuminating benzo[a]carbazole is a promising electron donor to construct highly efficient solar cells.

The incident photon-to-current conversion efficiency (IPCE) spectra of **JY21**–**23** were performed to analyze the J_{sc} values (Figure 7). The terminals of the IPCE spectra of **JY21**–**23** were at 670, 710, and 740 nm, respectively, which were much broader than that of their absorption spectra in dichloromethane solutions. Compared to those of the other two dyes, the IPCE values of **JY23** were higher and broader, and **JY23** achieved over 60% IPCE values from 350 to 620 nm with a highest IPCE value of 84% at 470 nm. The highest IPCE value and broadest absorption range of **JY23** ensured its highest J_{sc} and PCE among the three dyes.

The furan-linked dye **JY22** exhibited a significantly improved efficiency (about 0.9%) compared to thiophene-linked dye **JY21**. This is mainly due to the broader UV–vis absorption spectrum and IPCE response of the dye **JY22**, as well as its higher open-circuit photovoltage, which is similar to the results reported previously.[29,31] Compared to the analogous dyes **JK24**, **K2**, and **CCT3A** (Figure 3), dyes **JY21**–**23** presented relatively higher IPCE values, which guaranteed higher J_{sc} and PCEs (Table 2) and illustrated that benzo[a]carbazole is an efficient donor group.

Electrochemical Impedance Spectroscopy. To elucidate the correlation of the photovoltage and the dyes, we then performed electrochemical impedance spectroscopy (EIS).[32−34] Figure 8 shows the Nyquist plots and Bode plots of **JY21**, **JY22**, and **JY23**, which were measured in the darkness under forward bias (−0.75 V) with a frequency region (0.1−100 K Hz). The larger semicircle in Nyquist plots corresponds to the interfacial charge transfer resistances (R_K) on the TiO_2/dyes/electrolyte interface.[35] A larger semicircle means a greater R_K, indicating a strongly reduced electron recombination, a smaller dark current, and a higher V_{oc}. We fitted the Nyquist plots using a

Table 2. Photovoltaic Performance of JY21–23, N719,[a] and the Analogous Dyes

dye	DL (nmol cm^{-2})	V_{oc} (mV)	J_{sc} (mA cm^{-2})	FF	PCE (%)
JY21	216	729	12.4	0.66	6.01
JY22	161	757	13.8	0.66	6.93
JY23	162	744	14.8	0.68	7.54
N719		740	17.2	0.63	7.99
JK24[27]		740	9.83	0.70	5.02
K2[28]		724	13.3	0.66	6.68
CCT3A[29]		710	11.3	0.71	5.69

[a]The active area of solar cells was 0.196 cm^2; DL was the amount of dye loading on the TiO_2 electrode. Commercial **N719** dye was applied for comparison.

DOI: 10.1021/am508400a
ACS Appl. Mater. Interfaces 2015, 7, 9015−9022

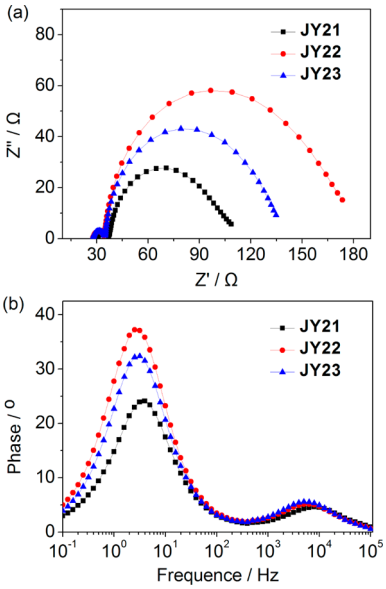

Figure 8. (a) Nyquist plots and (b) Bode plots for DSSCs based on **JY21**−**23** under −0.75 V bias.

diffusion−recombination model and an equivalent circuit according to the previous literatures.[36−38] The electrochemical impedance data of DSSCs sensitized with **JY21**−**23** are summarized in Table 3. The fitted R_K increased in the order

Table 3. Electrochemical Impedance Data of DSSCs Sensitized with JY21−23.[a]

dye	R_K (Ω)	R_W (Ω)	f (Hz)	K_{eff} (s^{-1})	τ (ms)	D_{eff} (cm^2 s^{-1})
JY21	61.8	0.140	3.98	25.0	40.0	0.011
JY22	126	0.145	2.51	15.8	63.4	0.014
JY23	92.2	0.102	3.16	19.8	50.4	0.018

[a] K_{eff} is the effective rate constant of recombination, $K_{eff} = 2\pi f$.

of **JY21** (61.8 Ω) < **JY23** (92.2 Ω) < **JY22** (126 Ω). This tendency is consistent with the order of V_{oc} of **JY21** (729 mV) < **JY23** (744 mV) < **JY22** (757 mV).

Electron lifetime (τ) can be calculated from the peak frequency (f) at lower frequency region in Bode plots using $\tau = 1/(2\pi f)$.[39] Generally, the relatively longer electron lifetime indicates an increased resistance of charge recombination, a reduced dark current, and an improved V_{oc}. The values of f decreased in the order of **JY21** > **JY23** > **JY22**, and the electron lifetime was enhanced in reverse with the values of **JY21** (40.0 ms) < **JY23** (50.4 ms) < **JY22** (63.4 ms). Thus, the relatively highest V_{oc} of **JY22** could be further explained. The effective electron diffusivity (D_{eff}) was calculated by $D_{eff} = (R_K/R_W)(L^2/\tau)$, in which R_W is the electron transport resistance in the photoanode, and L is the thickness of the TiO_2 film.[40−43] The D_{eff} value increased from 0.011 (**JY21**) to 0.014 (**JY22**) to 0.018 cm^2 s^{-1} (**JY23**), which is also in agreement with the order of DSSC performances.

CONCLUSIONS

Three novel benzo[*a*]carbazole-based organic dyes containing different π-linkers such as thiophene (**JY21**), furan (**JY22**), and oligothiophene (**JY23**), have been designed and synthesized for DSSCs. These dyes all exhibited the ability of highly efficient solar-to-electricity conversion, and their photophysical, electrochemical, and photovoltaic properties were found to be sensitive to the π-linkers. Notably, the dye **JY23** showed a broad IPCE response with a photocurrent signal up to about 740 nm, and a DSSC based on **JY23** gave the best photovoltaic performance with a J_{sc} of 14.8 mA cm^{-2}, a V_{oc} of 744 mV, a FF of 0.68, and an overall power conversion efficiency of 7.54% under AM 1.5 G irradiation. This result reveals that benzo[*a*]carbazole is a promising electron donor to construct effective organic dyes for DSSCs.

EXPERIMENTAL SECTION

Materials and Characterization Techniques. All solvents were purified using standard techniques. ^1H and ^{13}C NMR spectra, UV−visible absorption spectra, HR-MS spectra, cyclic voltammogram, and electrochemical impedance spectroscopy were measured according to previous methods.[44]

Fabrications and Measurements of Solar Cells. The preparation of the TiO_2 photoanodes and counter electrodes, as well as the fabrication and measurement of solar cells, was performed according to previous work.[45] The TiO_2 photoanodes were immersed in 0.3 mM **N719** (Solaronix SA, Switzerland) dye solution in ethanol for 12 h. The adsorption of the benzo[*a*]carbazole-based dyes on TiO_2 was carried out in 0.3 mM dye solution in THF for 12 h. The amounts of dye loading were determined by dye desorption into a basic solution (0.1 M NaOH in THF/H_2O = 1:1) followed by spectroscopic measurement. The liquid iodine electrolyte consisted of 0.3 M DMPII, 0.1 M LiI, 0.05 M I_2, and 0.5 M 4-*tert*-butylpyridine in CH_3CN.

Synthesis of Compound 4. A mixture of compound **2** (1.38 g, 3.15 mmol), bis(pinacolato)diboron (1.12 g, 4.73 mmol), potassium acetate (1.81 g, 18.5 mmol), and Pd(dppf)Cl_2·CH_2Cl_2 (0.18 g, 0.22 mmol) in 1,4-dioxane (25 mL) was stirred and heated at 85 °C for 4 h under a nitrogen atmosphere. After the solvent was removed, the mixture was redissolved in CH_2Cl_2 and washed thrice with water. After being dried by anhydrous Na_2SO_4, the solvent was removed, and the crude product was isolated by silica-gel column chromatography using CH_2Cl_2 as the eluent to give compound **4** as a colorless liquid (yield: 81.5%). ^1H NMR (400 MHz, $CDCl_3$) δ 9.24 (d, *J* = 8.0 Hz, 1H), 8.95 (s, 1H), 8.57 (d, *J* = 8.3 Hz, 1H), 7.80 (s, 1H), 7.71 (t, *J* = 7.3 Hz, 1H), 7.66 (t, *J* = 7.3 Hz, 1H), 7.43 (d, *J* = 8.9 Hz, 1H), 7.20 (d, *J* = 8.8 Hz, 1H), 4.68−4.42 (m, 2H), 4.07 (s, 3H), 2.39−2.20 (m, 1H), 1.44−1.22 (m, 8H), 1.01−0.85 (m, 6H). ^{13}C NMR (101 MHz, $CDCl_3$) δ 154.32, 137.43, 137.18, 136.44, 130.29, 130.07, 125.03, 124.59, 123.34, 122.74, 122.45, 118.76, 114.59, 110.86, 101.56, 83.56, 55.97, 53.55, 50.10, 39.64, 30.66, 28.61, 25.12, 23.99, 23.13, 14.14, 10.93. HR-MS (MALDI): *m*/*z* $[M]^+$ calcd for $C_{31}H_{40}BNO_3$, 485.3101; found, 485.3098.

Synthesis of Compound 5. Under a nitrogen atmosphere, a mixture of compound **4** (700 mg, 1.60 mmol), 5-formylfuran-2-boronic acid (274 mg, 1.76 mmol), Pd(dppf)Cl_2·CH_2Cl_2 (105 mg, 0.13 mmol), K_2CO_3 (730 mg, 2.30 mmol) in toluene (25 mL), and methanol (5 mL) was stirred and heated at reflux for 5 h before it was poured into water. The organic phase was separated and dried by anhydrous Na_2SO_4. After the solvent was removed under vacuum, the residue was isolated by silica-gel column chromatography using CH_2Cl_2 as the eluent to give compound **5** as an orange liquid (yield: 77.2%). ^1H NMR (400 MHz, $CDCl_3$) δ 10.01 (s, 1H), 8.55 (d, *J* = 8.4 Hz, 1H), 8.37 (d, *J* = 7.6 Hz, 1H), 8.26 (s, 1H), 7.89 (d, *J* = 3.8 Hz, 1H), 7.64 (t, *J* = 7.6 Hz, 1H), 7.60−7.53 (m, 2H), 7.46−7.42 (m, 1H), 7.41 (d, *J* = 3.8 Hz, 1H), 7.16 (dd, *J* = 8.9, 2.4 Hz, 1H), 4.62−4.48 (m, 2H), 3.98 (s, 3H), 2.38−2.14 (m, 1H), 1.41−1.21 (m, 8H), 0.92−0.84 (m, 6H). ^{13}C NMR (101 MHz, $CDCl_3$) δ 182.90, 154.45, 154.33, 142.87, 136.85, 136.56, 135.56, 131.18, 128.59, 126.82, 125.42, 125.26, 122.90, 122.77, 122.63, 122.55, 122.24, 118.44, 115.04, 111.01, 101.26, 55.91, 50.14, 39.66, 30.58, 28.53, 23.90, 23.06, 14.04, 10.86. HR-MS (MALDI): *m*/*z* $[M]^+$ calcd for $C_{30}H_{31}NO_2S$, 469.2075; found, 469.2086.

Synthesis of Compound 6. The synthetic procedure was similar to that of compound **5**, and the residue was isolated by silica-gel

DOI: 10.1021/am508400a
ACS Appl. Mater. Interfaces 2015, 7, 9015−9022

column chromatography using CH_2Cl_2 as the eluent to give compound **6** as an orange liquid (yield: 74.3%). ^{1}H NMR (400 MHz, $CDCl_3$) δ 9.74 (s, 1H), 8.56−8.46 (m, 1H), 8.44−8.35 (m, 2H), 7.61−7.50 (m, 3H), 7.45 (d, J = 3.6 Hz, 1H), 7.32 (d, J = 9.0 Hz, 1H), 7.12 (dd, J = 8.9, 2.3 Hz, 1H), 6.89 (d, J = 3.6 Hz, 1H), 4.40−4.16 (m, 2H), 3.98 (s, 3H), 2.18−2.02 (m, 1H), 1.35−1.19 (m, 8H), 0.88−0.80 (m, 6H). ^{13}C NMR (101 MHz, $CDCl_3$) δ 177.04, 160.78, 154.37, 151.85, 136.46, 135.75, 130.17, 126.19, 125.46, 125.17, 124.03, 122.97, 122.73, 122.57, 121.74, 118.47, 118.20, 115.05, 111.20, 110.96, 101.23, 55.88, 49.90, 39.51, 30.56, 28.49, 23.91, 23.02, 14.03, 10.83. HR-MS (MALDI): m/z $[M]^+$ calcd for $C_{30}H_{31}NO_3$, 453.2304; found, 453.2310.

Synthesis of Compound 7. A mixture of compound **3** (239 mg, 0.41 mmol), compound **4** (300 mg, 0.62 mmol), aqueous 1 M K_2CO_3 (5 mL), and $Pd(PPh_3)_4$ (35 mg, 0.03 mmol) in THF (15 mL) was stirred and heated at reflux overnight under a nitrogen atmosphere. After the solvent was removed, the residue was redissolved in CH_2Cl_2 and washed thrice with water. After being dried by anhydrous Na_2SO_4, the solvent was removed under vacuum, and the crude product was isolated by silica-gel column chromatography using CH_2Cl_2 as the eluent to give compound **7** as a red liquid (yield: 88.2%). ^{1}H NMR (400 MHz, $CDCl_3$) δ 9.86 (s, 1H), 8.61 (d, J = 8.4 Hz, 1H), 8.52 (d, J = 7.3 Hz, 1H), 8.29 (s, 1H), 7.68−7.56 (m, 4H), 7.48 (d, J = 9.0 Hz, 1H), 7.31 (d, J = 3.8 Hz, 1H), 7.22 (d, J = 3.8 Hz, 1H), 7.20−7.11 (m, 2H), 4.76−4.60 (m, 2H), 3.99 (s, 3H), 2.96−2.83 (m, 4H), 2.34−2.24 (m, 1H), 1.83−1.70 (m, 4H), 1.55−1.31 (m, 28H), 0.93−0.84 (m, 12H). ^{13}C NMR (101 MHz, $CDCl_3$) δ 182.47, 154.20, 142.23, 141.26, 140.52, 140.18, 140.10, 139.08, 138.71, 136.60, 135.12, 134.24, 131.87, 130.67, 129.56, 127.86, 127.40, 125.95, 125.18, 124.92, 123.40, 123.02, 122.88, 122.52, 121.76, 118.60, 114.77, 110.91, 101.38, 55.90, 50.13, 39.72, 31.99, 31.96, 30.81, 30.64, 30.35, 29.83, 29.79, 29.62, 29.59, 29.57, 29.51, 29.43, 29.36, 28.59, 23.95, 23.11, 22.78, 22.77, 14.21, 14.08, 10.90. HR-MS (MALDI): m/z $[M]^+$ calcd for $C_{54}H_{67}NO_2S_3$, 857.4334; found, 857.4330.

Synthesis of Compound JY21. A mixture of compound **5** (420 mg, 0.89 mmol), cyanoacetic acid (170 mg, 2.1 mmol), ammonium acetate (280 mg, 3.6 mmol), and acetic acid (15 mL) was heated at reflux for 3 h under a nitrogen atmosphere. After being cooled to ambient temperature, it was precipitated by pouring into water. The resulting solid was collected by filtration and washed thoroughly with water. Then, the crude product was purified by silica-gel column chromatography using CH_2Cl_2/CH_3OH (15:1) as the eluent to give **JY21** as a deep red solid (yield: 86.7%). ^{1}H NMR (400 MHz, acetone-d_6) δ 8.76 (d, J = 8.5 Hz, 1H), 8.57 (s, 1H), 8.51 (s, 1H), 8.40 (d, J = 8.4 Hz, 1H), 8.13 (d, J = 3.8 Hz, 1H), 7.91 (d, J = 2.2 Hz, 1H), 7.80−7.68 (m, 2H), 7.68−7.61 (m, 1H), 7.57 (d, J = 3.8 Hz, 1H), 7.16 (dd, J = 9.0, 2.5 Hz, 1H), 4.84 (d, J = 7.4 Hz, 2H), 3.95 (s, 3H), 2.33−2.22 (m, 1H), 1.46−1.34 (m, 4H), 1.32−1.11 (m, 4H), 0.90 (t, J = 7.4 Hz, 3H), 0.81 (t, J = 7.2 Hz, 3H). ^{13}C NMR (101 MHz, acetone-d_6) δ 163.37, 154.74, 153.44, 146.28, 139.21, 136.72, 135.64, 135.43, 133.33, 131.09, 129.00, 126.56, 125.66, 125.49, 123.06, 122.96, 122.89, 122.46, 122.36, 118.74, 116.34, 115.22, 111.41, 101.46, 55.16, 49.81, 39.68, 30.25, 28.32, 23.62, 22.76, 13.28, 10.25. HR-MS (MALDI): m/z $[M]^+$ calcd for $C_{33}H_{32}N_2O_3S$, 536.2134; found, 536.2130.

Synthesis of Compound JY22. The synthetic procedure was similar to that of **JY21**, and the residue was isolated by silica-gel column chromatography using CH_2Cl_2/CH_3OH (15:1) as the eluent to give **JY22** as a dark red solid (yield: 70.2%). ^{1}H NMR (400 MHz, DMSO-d_6) δ 8.84 (s, 1H), 8.68 (t, J = 7.2 Hz, 2H), 7.98 (s, 1H), 7.81 (d, J = 2.3 Hz, 1H), 7.73 (dd, J = 13.2, 8.3 Hz, 2H), 7.69−7.64 (m, 1H), 7.47 (d, J = 3.5 Hz, 1H), 7.29 (d, J = 3.6 Hz, 1H), 7.14 (dd, J = 9.0, 2.4 Hz, 1H), 4.78 (d, J = 7.1 Hz, 2H), 3.90 (s, 3H), 2.13−1.98 (m, 1H), 1.34−1.06 (m, 8H), 0.79 (t, J = 7.3 Hz, 3H), 0.73 (t, J = 7.0 Hz, 3H). ^{13}C NMR (101 MHz, DMSO-d_6) δ 164.46, 157.99, 154.53, 148.62, 136.91, 135.42, 134.89, 129.71, 126.86, 126.36, 126.06, 123.33, 123.03, 122.69, 121.96, 121.93, 119.32, 119.28, 118.88, 118.67, 115.37, 112.29, 112.22, 102.06, 55.94, 49.88, 39.48, 30.14, 28.26, 23.66, 22.83, 14.18, 11.09. HR-MS (MALDI): m/z $[M]^+$ calcd for $C_{33}H_{32}N_2O_4$, 520.2362; found, 520.2360.

Synthesis of Compound JY23. The synthetic procedure was similar to that of **JY21**, and the residue was isolated by silica-gel column chromatography using CH_2Cl_2/CH_3OH (15:1) as the eluent to give **JY23** as a purple solid (yield: 81.8%). ^{1}H NMR (400 MHz, acetone-d_6) δ 8.74 (d, J = 8.4 Hz, 1H), 8.48 (d, J = 8.2 Hz, 1H), 8.39 (s, 2H), 7.87 (d, J = 8.2 Hz, 2H), 7.71 (t, J = 8.1 Hz, 2H), 7.61 (t, J = 7.5 Hz, 1H), 7.48 (d, J = 3.5 Hz, 1H), 7.36 (d, J = 3.6 Hz, 1H), 7.27 (s, 1H), 7.15 (d, J = 8.9 Hz, 1H), 4.84 (d, J = 7.1 Hz, 2H), 3.96 (s, 3H), 3.04−2.95 (m, 2H), 2.96−2.88 (m, 2H), 2.27 (s, 1H), 1.91−1.66 (m, 4H), 1.58−1.17 (m, 28H), 0.96−0.75 (m, 12H). ^{13}C NMR (101 MHz, acetone-d_6) δ 154.58, 145.91, 142.13, 140.86, 140.74, 140.41, 140.40, 138.50, 136.71, 134.95, 133.84, 133.27, 132.51, 131.64, 130.97, 130.94, 129.27, 128.46, 126.98, 126.40, 125.38, 125.07, 123.11, 123.05, 122.93, 122.78, 121.80, 118.74, 115.97, 114.95, 111.29, 101.43, 55.17, 49.81, 39.71, 31.75, 31.73, 30.50, 30.27, 30.00, 29.57, 29.43, 29.41, 29.37, 29.29, 29.22, 29.20, 29.18, 29.09, 28.98, 28.82, 28.79, 23.63, 22.77, 22.46, 13.49, 13.29, 10.26. HR-MS (MALDI): m/z $[M]^+$ calcd for $C_{57}H_{68}N_2O_3S_3$, 924.4392; found, 924.4390.

■ ASSOCIATED CONTENT

Supporting Information

NMR spectra of all new compounds. This material is available free of charge via the Internet at http://pubs.acs.org.

■ AUTHOR INFORMATION

Corresponding Authors

*E-mail: zhuyizhou@nankai.edu.cn.

*E-mail: jyzheng@nankai.edu.cn. Fax/Tel: +86-22-2350 5572.

Notes

The authors declare no competing financial interest.

■ ACKNOWLEDGMENTS

We thank the 973 Program (2011CB932502), NSFC (Nos: 21172126 and 21272123), and NFFTBS (No. J1103306) for their financial support.

■ REFERENCES

(1) O'Regan, B.; Grätzel, M. A Low-Cost, High-Efficiency Solar Cell Based on Dye-Sensitized Colloidal TiO_2 Films. *Nature* **1991**, *353*, 737−740.

(2) Hagfeldt, A.; Boschloo, G.; Sun, L.; Kloo, L.; Pettersson, H. Dye-Sensitized Solar Cells. *Chem. Rev.* **2010**, *110*, 6595−6663.

(3) Nazeeruddin, M. K.; De Angelis, F.; Fantacci, S.; Selloni, A.; Viscardi, G.; Liska, P.; Ito, S.; Bessho, T.; Grätzel, M. Combined Experimental and DFT-TDDFT Computational Study of Photoelectrochemical Cell Ruthenium Sensitizers. *J. Am. Chem. Soc.* **2005**, *127*, 16835−16847.

(4) Yella, A.; Lee, H.-W.; Tsao, H. N.; Yi, C.; Chandiran, A. K.; Nazeeruddin, M. K.; Diau, E. W.-G.; Yeh, C.-Y.; Zakeeruddin, S. M.; Grätzel, M. Porphyrin-Sensitized Solar Cells with Cobalt (II/III) Based Redox Electrolyte Exceed 12% Efficiency. *Science* **2011**, *334*, 629−634.

(5) Yella, A.; Mai, C.-L.; Zakeeruddin, S. M.; Chang, S.-N.; Hsieh, C.-H.; Yeh, C.-Y.; Grätzel, M. Molecular Engineering of Push-Pull Porphyrin Dyes for Highly Efficient Dye-Sensitized Solar Cells: The Role of Benzene Spacers. *Angew. Chem., Int. Ed.* **2014**, *53*, 2973−2977.

(6) Mathew, S.; Yella, A.; Gao, P.; Humphry-Baker, R.; Curchod, B. F. E.; Ashari-Astani, N.; Tavernelli, I.; Rothlisberger, U.; Nazeeruddin, M. K.; Grätzel, M. Dye-Sensitized Solar Cells with 13% Efficiency Achieved through the Molecular Engineering of Porphyrin Sensitizers. *Nat. Chem.* **2014**, *6*, 242−247.

(7) Liang, M.; Chen, J. Arylamine Organic Dyes for Dye-Sensitized Solar Cells. *Chem. Soc. Rev.* **2013**, *42*, 3453−3488.

(8) Prachumrak, N.; Pojanasopa, S.; Namuangruk, S.; Kaewin, T.; Jungsuttiwong, S.; Sudyoadsuk, T.; Promarak, V. Novel Bis[5-(fluoren-2-yl)thiophen-2-yl]benzothiadiazole End-Capped with Carbazole Dendrons as Highly Efficient Solution-Processed Nondoped Red

DOI: 10.1021/am508400a
ACS Appl. Mater. Interfaces 2015, 7, 9015−9022

Emitters for Organic Light-Emitting Diodes. *ACS Appl. Mater. Interfaces* **2013**, *5*, 8694−8703.
(9) Li, J.; Li, Q.; Liu, D. Novel Thieno-[3,4-*b*]-Pyrazines Cored Dendrimers with Carbazole Dendrons: Design, Synthesis, and Application in Solution-Processed Red Organic Light-Emitting Diodes. *ACS Appl. Mater. Interfaces* **2011**, *3*, 2099−2107.
(10) Li, J.; Grimsdale, A. C. Carbazole-Based Polymers for Organic Photovoltaic Devices. *Chem. Soc. Rev.* **2010**, *39*, 2399−2410.
(11) Qian, X.; Zhu, Y.-Z.; Song, J.; Gao, X.-P.; Zheng, J.-Y. New Donor−π−Acceptor Type Triazatruxene Derivatives for Highly Efficient Dye-Sensitized Solar Cells. *Org. Lett.* **2013**, *15*, 6034−6037.
(12) Feng, Q.; Zhang, Q.; Lu, X.; Wang, H.; Zhou, G.; Wang, Z.-S. Facile and Selective Synthesis of Oligothiophene-Based Sensitizer Isomers: An Approach toward Efficient Dye-Sensitized Solar Cells. *ACS Appl. Mater. Interfaces* **2013**, *5*, 8982−8990.
(13) Marotta, G.; Reddy, M. A.; Singh, S. P.; Islam, A.; Han, L.; De Angelis, F.; Pastore, M.; Chandrasekharam, M. Novel Carbazole-Phenothiazine Dyads for Dye-Sensitized Solar Cells: A Combined Experimental and Theoretical Study. *ACS Appl. Mater. Interfaces* **2013**, *5*, 9635−9647.
(14) Thongkasee, P.; Thangthong, A.; Janthasing, N.; Sudyoadsuk, T.; Namuangruk, S.; Keawin, T.; Jungsuttiwong, S.; Promarak, V. Carbazole-Dendrimer-Based Donor−π−Acceptor Type Organic Dyes for Dye-Sensitized Solar Cells: Effect of the Size of the Carbazole Dendritic Donor. *ACS Appl. Mater. Interfaces* **2014**, *6*, 8212−8222.
(15) Venkateswararao, A.; Thomas, K. R. J.; Lee, C.-P.; Li, C.-T.; Ho, K.-C. Organic Dyes Containing Carbazole as Donor and π-Linker: Optical, Electrochemical, and Photovoltaic Properties. *ACS Appl. Mater. Interfaces* **2014**, *6*, 2528−2539.
(16) Wang, Z.; Wang, H.; Liang, M.; Tan, Y.; Cheng, F.; Sun, Z.; Xue, S. Judicious Design of Indoline Chromophores for High-Efficiency Iodine-Free Dye-Sensitized Solar Cells. *ACS Appl. Mater. Interfaces* **2014**, *6*, 5768−5778.
(17) Wang, Z.; Liang, M.; Wang, L.; Hao, Y.; Wang, C.; Sun, Z.; Xue, S. New Triphenylamine Organic Dyes Containing Dithieno[3,2-*b*:2′,3′-*d*]pyrrole (DTP) Units for Iodine-Free Dye-Sensitized Solar Cells. *Chem. Commun.* **2013**, *49*, 5748−5750.
(18) Zhang, M.; Wang, Y.; Xu, M.; Ma, W.; Li, R.; Wang, P. Design of High-Efficiency Organic Dyes for Titania Solar Cells Based on the Chromophoric Core of Cyclopentadithiophene-Benzothiadiazole. *Energy Environ. Sci.* **2013**, *6*, 2944−2949.
(19) Li, W.; Wu, Y.; Zhang, Q.; Tian, H.; Zhu, W. D−A−π−A Featured Sensitizers Bearing Phthalimide and Benzotriazole as Auxiliary Acceptor: Effect on Absorption and Charge Recombination Dynamics in Dye-Sensitized Solar Cells. *ACS Appl. Mater. Interfaces* **2012**, *4*, 1822−1830.
(20) Baheti, A.; Thomas, K. R. J.; Lee, C.-P.; Li, C.-T.; Ho, K.-C. Organic Dyes Containing Fluoren-9-ylidene Chromophores for Efficient Dye-Sensitized Solar Cells. *J. Mater. Chem. A* **2014**, *2*, 5766−5779.
(21) Cai, N.; Wang, Y.; Xu, M.; Fan, Y.; Li, R.; Zhang, M.; Wang, P. Engineering of Push-Pull Thiophene Dyes to Enhance Light Absorption and Modulate Charge Recombination in Mesoscopic Solar Cells. *Adv. Funct. Mater.* **2013**, *23*, 1846−1854.
(22) Xiao, F.; Liao, Y.; Wu, M.; Deng, G.-J. One-Pot Synthesis of Carbazoles from Cyclohexanones and Arylhydrazine Hydrochlorides under Metal-Free Conditions. *Green Chem.* **2012**, *14*, 3277−3280.
(23) Tsuchimoto, T.; Matsubayashi, H.; Kaneko, M.; Nagase, Y.; Miyamura, T.; Shirakawa, E. Indium-Catalyzed Annulation of 2-Aryl- and 2-Heteroarylindoles with Propargyl Ethers: Concise Synthesis and Photophysical Properties of Diverse Aryl- and Heteroaryl-Annulated-[*a*]carbazoles. *J. Am. Chem. Soc.* **2008**, *130*, 15823−15835.
(24) Zhou, J.; Zuo, Y.; Wan, X.; Long, G.; Zhang, Q.; Ni, W.; Liu, Y.; Li, Z.; He, G.; Li, C.; Kan, B.; Li, M.; Chen, Y. Solution-Processed and High-Performance Organic Solar Cells Using Small Molecules with a Benzodithiophene Unit. *J. Am. Chem. Soc.* **2013**, *135*, 8484−8487.
(25) Qian, X.; Lu, L.; Zhu, Y.-Z.; Gao, H.-H.; Zheng, J.-Y. Triazatruxene-Based Organic Dyes Containing a Rhodanine-3-Acetic Acid Acceptor for Dye-Sensitized Solar Cells. *Dyes Pigm.* **2015**, *113*, 737−742.
(26) Kumar, D.; Thomas, K. R. J.; Lee, C.-P.; Ho, K.-C. Organic Dyes Containing Fluorene Decorated with Imidazole Units for Dye-Sensitized Solar Cells. *J. Org. Chem.* **2014**, *79*, 3159−3172.
(27) Kim, D.; Lee, J. K.; Kang, S. O.; Ko, J. Molecular Engineering of Organic Dyes Containing *N*-aryl Carbazole Moiety for Solar Cell. *Tetrahedron* **2007**, *63*, 1913−1922.
(28) He, J.; Hua, J.; Hu, G.; Yin, X. J.; Gong, H.; Li, C. Organic Dyes Incorporating a Thiophene or Furan Moiety for Efficient Dye-Sensitized Solar Cells. *Dyes Pigm.* **2014**, *104*, 75−82.
(29) Sudyoadsuk, T.; Pansay, S.; Morada, S.; Rattanawan, R.; Namuangruk, S.; Kaewin, T.; Jungsuttiwong, S.; Promarak, V. Synthesis and Characterization of D−D−π−A-Type Organic Dyes Bearing Carbazole-Carbazole as a Donor Moiety (D−D) for Efficient Dye-Sensitized Solar Cells. *Eur. J. Org. Chem.* **2013**, *2013*, 5051−5063.
(30) Gao, P.; Tsao, H. N.; Grätzel, M.; Nazeeruddin, M. K. Fine-Tuning the Electronic Structure of Organic Dyes for Dye-Sensitized Solar Cells. *Org. Lett.* **2012**, *14*, 4330−4333.
(31) Wan, Z.; Jia, C.; Duan, Y.; Zhou, L.; Lin, Y.; Shi, Y. Phenothiazine−Triphenylamine Based Organic Dyes Containing Various Conjugated Linkers for Efficient Dye-Sensitized Solar Cells. *J. Mater. Chem.* **2012**, *22*, 25140−25147.
(32) Mao, J.; He, N.; Ning, Z.; Zhang, Q.; Guo, F.; Chen, L.; Wu, W.; Hua, J.; Tian, H. Stable Dyes Containing Double Acceptors without COOH as Anchors for Highly Efficient Dye-Sensitized Solar Cells. *Angew. Chem., Int. Ed.* **2012**, *51*, 9873−9876.
(33) Cai, M.; Pan, X.; Liu, W.; Sheng, J.; Fang, X.; Zhang, C.; Huo, Z.; Tian, H.; Xiao, S.; Dai, S. Multiple Adsorption of Tributyl Phosphate Molecule at the Dyed-TiO_2/Electrolyte Interface to Suppress the Charge Recombination in Dye-Sensitized Solar Cell. *J. Mater. Chem. A* **2013**, *1*, 4885−4892.
(34) Chen, C.; Yang, X.; Cheng, M.; Zhang, F.; Zhao, J.; Sun, L. Efficient Panchromatic Organic Sensitizers with Dihydrothiazole Derivative as π-Bridge for Dye-Sensitized Solar Cells. *ACS Appl. Mater. Interfaces* **2013**, *5*, 10960−10965.
(35) Zhao, J.; Yang, X.; Cheng, M.; Li, S.; Sun, L. Molecular Design and Performance of Hydroxylpyridium Sensitizers for Dye-Sensitized Solar Cells. *ACS Appl. Mater. Interfaces* **2013**, *5*, 5227−5231.
(36) Yang, C.-H.; Lin, W.-C.; Wang, T.-L.; Shieh, Y.-T.; Chen, W.-J; Liao, S.-H.; Sun, Y.-K. Performance Variation from Triphenylamine- to Carbazole-Triphenylamine-Rhodaniline-3-Acetic Acid Dyes in Dye-Sensitized Solar Cells. *Mater. Chem. Phys.* **2011**, *130*, 635−643.
(37) Hsiao, H.-A.; Leu, C.-C.; Yang, C.-H.; Wang, T.-L.; Shieh, Y.-T. Binder-Addition Effect in TiO_2 Nanoparticles on Dye-Sensitized Solar Cells Evidenced by Spectroscopic Techniques. *Electrochim. Acta* **2013**, *111*, 784−790.
(38) Yang, C.-H.; Chen, P.-Y.; Chen, W.-J.; Wang, T.-L.; Shieh, Y.-T. Spectroscopic Evidences of Synergistic Co-Sensitization in Dye-Sensitized Solar Cells via Experimentation of Mixture Design. *Electrochim. Acta* **2013**, *107*, 170−177.
(39) Thomas, K. R. J.; Kapoor, N.; Lee, C.-P.; Ho, K.-C. Organic Dyes Containing Pyrenylamine-Based Cascade Donor Systems with Different Aromatic π Linkers for Dye-Sensitized Solar Cells: Optical, Electrochemical, and Device Characteristics. *Chem.—Asian J.* **2012**, *7*, 738−750.
(40) Adachi, M.; Sakamoto, M.; Jiu, J.; Ogata, Y.; Isoda, S. Determination of Parameters of Electron Transport in Dye-Sensitized Solar Cells Using Electrochemical Impedance Spectroscopy. *J. Phys. Chem. B* **2006**, *110*, 13872−13880.
(41) Yang, C.-H.; Liao, S.-H.; Sun, Y.-K.; Chuang, Y.-Y.; Wang, T.-L.; Shieh, Y.-T.; Lin, W.-C. Optimization of Multiple Electron Donor and Acceptor in Carbazole-Triphenylamine-Based Molecules for Application of Dye-Sensitized Solar Cells. *J. Phys. Chem. C* **2010**, *114*, 21786−21794.
(42) Fabregat-Santiago, F.; Bisquert, J.; Palomares, E.; Otero, L.; Kuang, D.; Zakeeruddin, S. M.; Grätzel, M. Correlation between Photovoltaic Performance and Impedance Spectroscopy of Dye-

DOI: 10.1021/am508400a
ACS Appl. Mater. Interfaces 2015, 7, 9015−9022

Sensitized Solar Cells Based on Ionic Liquids. *J. Phys. Chem. C* **2007**, *111*, 6550−6560.
(43) Bisquert, J.; Cahen, D.; Hodes, G.; Ruhle, S.; Zaban, A. Physical Chemical Principles of Photovoltaic Conversion with Nanoparticulate, Mesoporous Dye-Sensitized Solar Cells. *J. Phys. Chem. B* **2004**, *108*, 8106−8118.
(44) Qian, X.; Gao, H.-H.; Zhu, Y.-Z.; Lu, L.; Zheng, J.-Y. 6*H*-Indolo[2,3-*b*]quinoxaline-Based Organic Dyes Containing Different Electron-Rich Conjugated Linkers for Highly Efficient Dye-Sensitized Solar Cells. *J. Power Sources* **2015**, *280*, 573−580.
(45) Qian, X.; Gao, H.-H.; Zhu, Y.-Z.; Lu, L.; Zheng, J.-Y. Biindole-Based Double D−π−A Branched Organic Dyes for Efficient Dye-Sensitized Solar Cells. *RSC Adv.* **2015**, *5*, 4368−4375.

DOI: 10.1021/am508400a
ACS Appl. Mater. Interfaces 2015, 7, 9015−9022